Claudin-4 forms paracellular chloride channel in the kidney and requires claudin-8 for tight junction localization

Jianghui Hou[a,1], Aparna Renigunta[b], Jing Yang[a], and Siegfried Waldegger[b]

[a]Renal Division, Washington University Medical School, St. Louis, MO 63110; and [b]University Children's Hospital, Philipps University, 35043 Marburg, Germany

Edited by Maurice B. Burg, National Heart, Lung, and Blood Institute, Bethesda, MD, and approved September 13, 2010 (received for review June 29, 2010)

Tight junctions (TJs) play a key role in mediating paracellular ion reabsorption in the kidney. The paracellular pathway in the collecting duct of the kidney is a predominant route for transepithelial chloride reabsorption that determines the extracellular NaCl content and the blood pressure. However, the molecular mechanisms underlying the paracellular chloride reabsorption in the collecting duct are not understood. Here we showed that in mouse kidney collecting duct cells, claudin-4 functioned as a Cl^- channel. A positively charged lysine residue at position 65 of claudin-4 was critical for its anion selectivity. Claudin-4 was observed to interact with claudin-8 using several criteria. In the collecting duct cells, the assembly of claudin-4 into TJ strands required its interaction with claudin-8. Depletion of claudin-8 resulted in the loss of paracellular chloride conductance, through a mechanism involving its recruitment of claudin-4 during TJ assembly. Together, our data show that claudin-4 interacts with claudin-8 and that their association is required for the anion-selective paracellular pathway in the collecting duct, suggesting a mechanism for coupling chloride reabsorption with sodium reabsorption in the collecting duct.

ion channel | chloride shunt | blood pressure | siRNA | protein interaction

Chloride is the predominant extracellular ionic constituent and thereby determines extracellular fluid volume (ECFV) and blood pressure (1–3). Although only responsible for the reabsorption of 2–3% filtered chloride, the aldosterone-sensitive distal nephron (ASDN) plays a vital regulatory role in renal handling of salt, ECFV control, and managing blood pressure (4). The ASDN comprises the distal convoluted tubule (DCT), the connecting tubule (CNT), and the collecting duct. The collecting duct is characterized by a heterogeneous epithelium—the principal cells and intercalated cells (5). Sodium reabsorption in the collecting duct is an active process driven by the basolateral Na^+/K^+-ATPase; acts through the apical epithelial sodium channel (ENaC) in the principal cell (6); and is responsible for generating the lumen-negative transepithelial potential. This electrogenic transport step creates a favorable electrical driving force for luminal reabsorption of chloride and secretion of potassium and proton. Chloride is transported by two major mechanisms (1). Chloride is actively reabsorbed by an electroneutral Cl^-/HCO^- exchanger (*Slc26a4*: pendrin) localized to the apical membrane of the β-type intercalated cell (7). Choride exits this cell via a basolateral Cl^- channel (2) and diffuses passively down electrochemical gradients via the paracellular channel in the tight junction (TJ).

The TJ is the most apical member of the junctional complex found in vertebrate epithelia responsible for the barrier to movement of ions and molecules between apical and basal compartments, the paracellular pathway (8). TJs are composed of three transmembrane proteins: occludin, claudins, and junctional adhesion molecule (JAM). The claudins (CLDNs) are a 28-member family of tetraspan proteins that range in molecular mass from 20 to 28 kDa (9). In renal epithelia, claudins have been shown to form the paracellular channel, a novel class of channels oriented perpendicular to the membrane plane and serving to join two extracellular compartments (10). The paracellular channel is similar to the conventional transmembrane channels in many features, such as small pore apertures (of radius <4 Å), properties of ion selectivity, pH dependence, and anomalous mole fraction effects (11).

The expression pattern of claudins varies considerably in the kidney. CLDN3, 4, 7, and 8 are expressed primarily along the ASDN (12–14). In cultured renal epithelial MDCK cells, CLDN4 or CLDN8 overexpression selectively decreased the permeability of cations through TJs, specifically to Na^+, K^+, H^+, and ammonium (15, 16). CLDN7 overexpression in LLC-PK1 cells increased paracellular permeability to Na^+ and decreased paracellular permeability to Cl^- (17). However, these surrogate tissue-culture models are of the proximal tubule origin, and with claudin expression profile different from that of the collecting duct. Any permeability change recorded in these cells reflects the combined function of both endogenous and exogenous claudins. To faithfully interpret claudin function in the collecting duct, we have generated in vitro cultures of claudin-deficient collecting duct cells using RNA interference. By manipulating endogenous claudin expression and recording ion permeability changes, we provide evidence that CLDN4 forms a paracellular chloride channel in the collecting duct, and identify a locus of amino acids critical for its function.

Claudins *cis* interact within the plane of the membrane to form dimers, or higher oligomeric state, followed by *trans* interactions between claudins in adjacent cells and additional *cis* interactions to assemble claudin oligomers into intramembrane TJ strands (18). Claudin knockdown experiments in transgenic animals revealed that the *cis* interaction between CLDN16 and CLDN19 was required for their assembly into TJ strands (19). Here, we observed the physical interaction between CLDN4 and CLDN8 using several criteria. In the collecting duct cells, the assembly of CLDN4 into TJ strands required its interaction with CLDN8. Depletion of CLDN8 resulted in the loss of paracellular chloride conductance, through a mechanism involving its recruitment of CLDN4 during TJ assembly. Neither loss of CLDN4 nor CLDN8 affected the junctional localization of CLDN3 or CLDN7, the normal constituents of TJ in the collecting duct. Together, these data suggest that CLDN4 and CLDN8 interact and are required for the anion-selective paracellular channel in the collecting duct.

Results

RNAi Depletion of CLDN4 and CLDN8 in the Collecting Duct Cells. Using antibodies available to us, we screened for collecting duct localization of claudins in the mouse kidney and found CLDN4 and 8 expression in the collecting duct (Fig. S1*A*). Double-immunofluorescence staining showed exclusive colocalization of CLDN4 with CLDN8 in both cortical and medullar collecting

Author contributions: J.H. designed research; J.H., A.R., and J.Y. performed research; J.H., A.R., and S.W. analyzed data; and J.H. wrote the paper.

The authors declare no conflict of interest.

This article is a PNAS Direct Submission.

[1]To whom correspondence should be addressed. E-mail: jhou@wustl.edu.

This article contains supporting information online at www.pnas.org/lookup/suppl/doi:10.1073/pnas.1009399107/-/DCSupplemental.

ducts (Fig. S1*B*). Cultured mouse collecting duct cells (e.g., the cortical collecting duct cell M-1 and the inner medullar collecting duct cell mIMCD3) retain most of the in vivo physiological features of the collecting duct, such as expression of the amiloride-sensitive epithelial Na^+ channel (ENaC) and many components of the aldosterone signaling pathway (including sgk1) (20, 21). Both cell lines express endogenous CLDN4 and CLDN8. We previously described a method of knocking down endogenous claudin gene expression in cultured epithelial cells using RNA interference (22). The short interference oligonucleotides (siRNAs) were designed and cloned with the strategy described previously (22). Each siRNA oligonucleotide contains a unique complementary 19-nucleotide sequence within the coding region of mouse claudin gene. As we aimed to have claudin expression suppressed by siRNAs during a prolonged period in cultured collecting duct cells, so that they could become fully polarized and form TJs (normally >7 d), we used a previously described retroviral siRNA expression system (pSIREN; *Methods*) to generate the VSV-G pseudotyped retrovirus (titer used at 1×10^6 cfu/mL) capable of infecting a wide range of cell types and integrating into the host genome (22, 23). Each individual siRNA construct was used to infect mouse collecting duct cells (with empty vector-infected cells as control), and the infected cells were seeded onto Transwell inserts to become polarized. On day 9 postpolarization, cell monolayers were subjected to electrophysiological measurements and immunostaining assays to determine the effectiveness of each siRNA construct in suppression of claudin gene expression. Ten to 15 siRNA sequences spanning the gene coding region of CLDN4 and CLDN8 were screened; only a small number of siRNA sequences suppressed both detectable staining on Western blots (Fig. S2*A*) and detectable immunofluorescence labeling (>90% loss; Fig. S2*B*). Two sequences with these activities were identified for CLDN4 (282 and 379), and three for CLDN8 (246, 512, and 714; Table S1). For each effective siRNA construct, two independent infections were studied in each cell line, and measurements were performed in triplicate for each independent experiment.

CLDN4 Is a Paracellular Cl^- Channel. The collecting duct is considered a tight epithelium with high transepithelial resistance (TER > 500 $\Omega \cdot cm^2$) (24), whereas other segments of the nephron, such as the proximal tubule and the thick ascending limb, are leaky (TER < 100 $\Omega \cdot cm^2$). In collecting duct cell monolayers with high TER, such as M-1 and mIMCD3 cells, the transepithelial ion conductance can be attributed to two separate pathways: transcellular and paracellular pathways. We used a mixture of transmembrane ion channel inhibitors to block transcellular ion conductance (*Methods*; amiloride for the epithelial Na^+ channel, bumetanide for the Na^+-K^+-2 Cl^- cotransporter, DIDS for anion exchangers, and NFA for pendrin). Any recorded change in transepithelial ion conductance was therefore mediated through the paracellular channels. In M-1 cells, CLDN4 knockdown (KD) using the siRNA construct 282 significantly increased the TER by 27% (KD: 809.0 ± 10.2 vs. control; 635.3 ± 20.8 $\Omega \cdot cm^2$, $P < 0.01$, $n = 3$; Table 1). Current–voltage curves were linear in the presence and absence of siRNA, consistent with a paracellular ion conductance. Dilution potentials were measured to determine the ion selectivity across the M-1 monolayers (with the apical side as zero reference; *Methods*). Determinants of the dilution potential include the dilution factor of the applied transepithelial NaCl gradient and the ion permeability ratio (P_{Cl}/P_{Na}). CLDN4-siRNA 282 significantly increased the dilution potential of control M-1 cells (0.97 ± 0.12 mV) to 3.90 ± 0.15 mV ($P < 0.01$, $n = 3$). The Goldman–Hodgkin–Katz equation calculated the ion permeability ratio (P_{Cl}/P_{Na}) at 0.878 ± 0.014 in control cells compared with 0.585 ± 0.013 in CLDN4 KD cells ($P < 0.01$, $n = 3$; Table 1). This decrease in P_{Cl}/P_{Na} was attributable to a 38% decrease in absolute P_{Cl} (control: 1.351 ± 0.012 vs. KD: 0.837 ± 0.012 × 10^{-6} cm/s, $P < 0.01$, $n = 3$; Table 1), whereas P_{Na} displayed no significant change. The effects of CLDN4 KD were more pronounced in mIMCD3 cells. CLDN4-siRNA 282 markedly increased the dilution potential in mIMCD3 cells to 8.00 ± 0.17 mV (compared with 1.97 ± 0.09 mV in control cells, $P < 0.01$, $n = 3$; Table 1). P_{Cl}/P_{Na} in KD cells were significantly reduced (KD: 0.303 ± 0.010 vs. control: 0.766 ± 0.009, $P < 0.01$, $n = 3$), owing to a 65% decrease in absolute P_{Cl} (KD: 0.582 ± 0.014 vs. control: 1.672 ± 0.011 ×10^{-6} cm/s, $P < 0.01$, $n = 3$; Table 1). A second siRNA construct (379) for CLDN4 KD independently confirmed the effects of 282 in both M-1 and mIMCD3 cells. The ineffective CLDN4 siRNA sequence (348) showed no significant effect on P_{Cl} or P_{Na} in M-1 and mIMCD3 cells (Table S3), ruling out any off-target effect of RNA interference on paracellular ion permeation.

Because CLDN4 mediated P_{Cl} (ΔP_{Cl}: P_{Cl} in control – P_{Cl} in KD) is notably greater in mIMCD3 cells, further analyses of CLDN4 channel properties were carried out in mIMCD3 cells. To estimate the electrostatic interaction strength between permeating anions and the CLDN4 channel pore, we determined the permeability of CLDN4 to a run of halide anions with different ionic radii using biionic potentials (Table S2). The permeability sequence was found to be: $Br^- > Cl^- \sim I^- > F^-$. This sequence is different from the sequence of their free-solution mobilities (Eisenman series I: $I^- > Br^- > Cl^- > F^-$) but resembles the Eisenman selectivity sequence III, indicating a moderate electrical field strength within the channel pore that now favors small, dehydrated halides for passage (25). This explained the selectivity of CLDN4 for anion over cation. However, the difference between the permeabilities of the most permeable halide anion (Br^-) and the least permeable (F^-) was small, by 1.23-fold, indicating CLDN4 is a nonselective anion channel with partially hydrated channel pore.

To provide evidence that the observed CLDN4 channel is selective for ion permeation, we measured the paracellular permeability for the noncharged solute, mannitol (mol wt 182; radius 3.6 Å), across mIMCD3 cell monolayers (*Methods*). The mannitol permeability in CLDN4 KD cells was not significantly different from that in control cells (Table S4), indicating CLDN4 is not required for the paracellular flux of macromolecules.

Mutagenesis Identifies a Locus of Amino Acids Critical for CLDN4 Ion Selectivity. The paracellular channel pores use intrapore electrostatic binding sites to achieve a high conductance with a high degree of ion selectivity. Ion selectivity is mediated by the electrostatic interaction of partially dehydrated permeating ions with charged sites within the pore. It is generally accepted that the charges on the first extracellular loops (ECL1) of claudins line the channel pores and electrostatically influence passage of soluble

Table 1. Paracellular ion conductance in collecting duct cells depleted with claudins

Group	TER, $\Omega \cdot cm^2$	Dilution potential, mV	P_{Cl}/P_{Na}	P_{Cl}, 10^{-6} cm/s	P_{Na}, 10^{-6} cm/s
M-1	635.3 ± 20.8	0.97 ± 0.12	0.878 ± 0.014	1.351 ± 0.012	1.539 ± 0.012
M-1:cldn4-siRNA	809.0 ± 10.2	3.90 ± 0.15	0.585 ± 0.013*	0.837 ± 0.012*	1.432 ± 0.012
M-1:cldn8-siRNA	768.3 ± 30.6	3.47 ± 0.18	0.622 ± 0.016*	0.916 ± 0.014*	1.473 ± 0.014
mIMCD3	476.3 ± 27.8	1.97 ± 0.09	0.766 ± 0.009	1.672 ± 0.011	2.184 ± 0.011
mIMCD3:cldn4-siRNA	732.7 ± 18.7	8.00 ± 0.17	0.303 ± 0.010†	0.582 ± 0.014†	1.922 ± 0.014
mIMCD3:cldn8-siRNA	656.3 ± 13.5	6.93 ± 0.28	0.366 ± 0.017†	0.762 ± 0.027†	2.084 ± 0.027
mIMCD3:cldn3-siRNA	497.7 ± 8.1	1.83 ± 0.09	0.780 ± 0.009	1.615 ± 0.011	2.070 ± 0.011
mIMCD3:cldn7-siRNA	333.0 ± 23.5	2.37 ± 0.03	0.725 ± 0.003	2.316 ± 0.006‡	3.195 ± 0.006‡

CLDN4-siRNA: 282; CLDN8-siRNA: 512; CLDN3-siRNA: 471; CLDN7-siRNA: 772.

*$P < 0.01$ relative to control M-1 cells, $n = 3$.

†$P < 0.01$ relative to control mIMCD3 cells, $n = 3$.

‡$P < 0.01$ relative to control mIMCD3 cells, $n = 3$.

CELL BIOLOGY

ions (26). The ECL1 of CLDN4 is enriched with six charged amino acids; among them, three basic residues (R31, K65, and R81; Fig. 1*A*) are interspersed with three acidic residues (E48, D68, and D76; Fig. 1*A*). To identify the pore-lining residues critical for CLDN4 anion selectivity, we have systematically removed the charge from each of the six charged amino acids by mutagenesis (D→N; E→Q; K,R→T) and studied the effects of charge removal upon the function of CLDN4 in mIMCD3 cells. The endogenous CLDN4 expression in mIMCD3 cells was depleted with siRNA (282) and subsequently rescued with the siRNA-resistant human isoform of CLDN4 (WT or its mutants), which contains six mismatches to the mouse siRNA sequence. To normalize the expression among various CLDN4 mutants and with the WT, we used a previously described retroviral expression method to transfect transgenes into mIMCD3:CLDN4-siRNA cell background with a fixed titer of retrovirus at 1×10^6 CFU/mL (23), and quantified the transcription of transgenes by RT-PCR. On day 9 following the development of polarized monolayers, the Transwell filters were subjected to electrophysiological measurements and subsequently immunostained to visualize rescued CLDN4 expression. To more rigorously determine the expression levels and the localization patterns of CLDN4 mutants, we have transfected GFP-tagged CLDN4 mutant proteins into mIMCD3:CLDN4-siRNA cells. Of the six mutant proteins, R81T was weakly expressed by cells (Fig. S3*A*) and confined to the ER (Fig. S3*B*), likely caused by protein misfolding defects. The rest of the mutant proteins were expressed at a comparable level to the WT (Fig. S3*A*), and all localized to the TJ (Fig. S3*B* and Table 2). Ectopic expression of GFP-tagged human CLDN4 mutant proteins did not perturb the silencing effect of siRNA-282; endogenous expression of mouse CLDN4 protein was continuously suppressed in mIMCD3 cells (Fig. S3*A*). Because fused GFP moiety may interfere with claudin channel functions, untagged human CLDN4 proteins (WT and its mutants) were used for rescuing paracellular Cl^- conductance in mIMCD3:CLDN4-siRNA cells (vide infra).

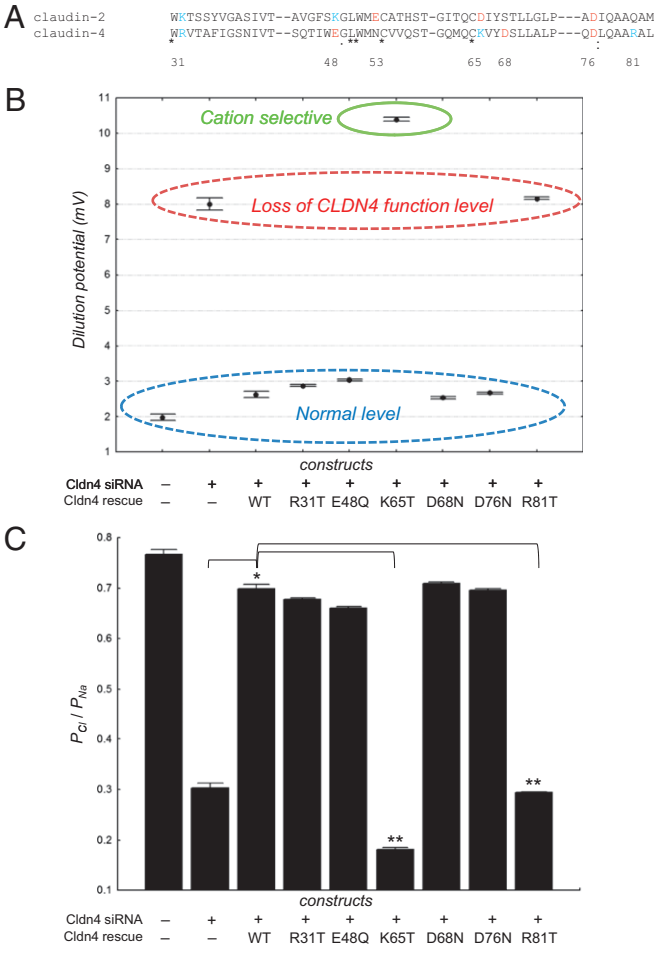

Fig. 1. Effects of CLDN4 and its charge-neutralizing mutants in mIMCD3 cells on paracellular ion conductance. (*A*) Amino acid sequence alignment of the first extracellular loops of CLDN2 and CLDN4. Negatively charged amino acids are labeled in red; positively charged amino acids are in blue. Note the charge of amino acid differs at the position 65 of CLDN4 from CLDN2. Dilution potential values (*B*) and P_{Cl}/P_{Na} (*C*) across mIMCD3 cell monolayers expressing mouse CLDN4-siRNA (282), human WT CLDN4 and its mutants, individually or in pairs, are shown. $*P < 0.01$ relative to CLDN4-siRNA, $n = 3$; $**P < 0.01$ relative to CLDN4-WT, $n = 3$.

The WT CLDN4 increased the ion permeability ratio (P_{Cl}/P_{Na}) in mIMCD3:CLDN4-siRNA cells (WT: 0.699 ± 0.009 vs. KD: 0.303 ± 0.010, $P < 0.01$, $n = 3$; Table 2 and Fig. 1*C*), resulting in the return of the dilution potential to its base line (Fig. 1*B*). The elevated TER in KD cells (732.7 ± 18.7 Ω·cm^2) was restored to near the control level (410.0 ± 3.8 Ω·cm^2) by WT CLDN4, indicating CLDN4 forms a paracellular Cl^- channel (P_{Cl}, WT: 1.841 ± 0.013 vs. KD 0.582 ± 0.014 ×10^{-6} cm/s, $P < 0.01$, $n = 3$). Neutralizing the negative charges in CLDN4 ECL1 (E48Q, D68N, and D76N) had no significant effects on CLDN4 function. Expression of these mutants in KD cells increased P_{Cl} to near the WT level (Table 2), which indicates that the ion selectivity of CLDN4 channel is not related to the charge density in ECL1 but mediated through specific electrostatic binding sites. Charge neutralization on basic residue K65 but not R31abolished CLDN4 function. Expression of K65T in KD cells failed to increase P_{Cl} (Table 2). Notably, the dilution potential was further increased by K65T in KD cells to 10.40 ± 0.06 mV (Fig. 1*B*), accompanied by a significant decrease in TER (K65T: 389.0 ± 4.7 vs. KD: 732.7 ± 18.7 Ω·cm^2, $P < 0.01$, $n = 3$; Table 2). The Kimizuka–Koketsu equation calculated P_{Na} and found it was significantly increased by K65T mutation (K65T: 3.990 ± 0.009 vs. WT: 2.635 ± 0.013 ×10^{-6} cm/s, $P < 0.01$, $n = 3$; Table 2). Thus, K65 is required for maximum anion permeability of CLDN4 and for the electrostatic interaction site in the CLDN4 channel pore. The ionic amine group on this lysine stabilizes permeating anions but shields off cations, according to Coulomb's law. Loss of the positive charge reversed the ion selectivity of CLDN4 to becoming slightly permeable to cations (Fig. 1*B*; *Discussion*). Yu et al. (27) have studied the CLDN2 channel in MDCK cells and identified an acidic residue, aspartate, at the homologous position 65 (Fig. 1*A*), critical for its cation selectivity.

CLDN8 Is Critical for Paracellular Cl^- Permeability. In both M-1 and mIMCD3 cells, CLDN8 KD significantly decreased the Cl^- permeability (P_{Cl}) by 32% and 54%, respectively (Table 1), to a similar level as in CLDN4 KD. The Na^+ permeability (P_{Na}) was not affected by CLDN8 KD, resulting in a significant loss of anion selectivity (P_{Cl}/P_{Na}) in M-1 and mIMCD3 cells (Table 1). Table 1 summarizes the findings of CLDN8 KD using siRNA 512, which were independently confirmed by two other siRNAs, 246 and 714. The permeation of noncharged molecule (mannitol) was not dependent on CLDN8 (Table S4). Thus, CLDN8 is required for the paracellular Cl^- channel in the collecting duct. Immunofluorescence analyses have shown that CLDN3 and 7 are also expressed in the collecting ducts of mouse and rat kidneys (12, 14), although one study described CLDN7 in the collecting ducts as located primarily on the basolateral membrane (13). Both M-1 and mIMCD3 cells express endogenous CLDN3 and CLDN7. We asked whether the paracellular Cl^- permeability was mediated selectively through CLDN4 and CLDN8, or a collective effect requiring multiple claudin interactions. Using RNA interference, we have knocked down CLDN3 and CLDN7 expression in M-1 and mIMCD3 cells (Table S1). CLDN3 KD had no significant effect on P_{Cl} or P_{Na} (mIMCD3 cells shown as representative; Table 1). CLDN7 KD resulted in a 30% decrease in TER but no significant change in ion selectivity (P_{Cl}/P_{Na}; siRNA 772 shown as representative; Table 1), indicating a TJ barrier-function defect. This is consistent with the in vivo findings that CLDN7 KO animal kidneys lose major extracellular ions, such as Na^+, K^+, and Cl^-, in a similar rate (14). Our findings suggest that the paracellular Cl^- channel in the collecting duct is formed by CLDN4 and CLDN8, without involving CLDN3 or CLDN7.

CLDN8 Physically Interacts with CLDN4. Claudins interact with one another both intracellularly and intercellularly; they copolymerize linearly within the plasma membrane of the cell, together with the integral protein occludin, to form the intramembrane TJ strands (28). These intramembrane interactions (side-to-side) can involve one claudin protein (homomeric or homopolymeric) or different claudins (heteromeric or heteropolymeric). In the formation of the intercellular junction, claudins may interact head-to-head with claudins in an adjacent cell, generating both homotypic and heterotypic claudin-claudin interactions. In an earlier in vitro study, we have found CLDN16 and CLDN19 heteromeric interaction using several criteria (29). In vivo claudin knockdown (KD) experiments show that this CLDN16-19 interaction is required for their assembly into the TJ (19). If this interaction fails to occur, neither claudin can traffic correctly to the plasma membrane and cell junction. Therefore, the phenotypes of CLDN19 KD mice were highly similar to those reported for CLDN16 KD mice (19, 30). Functional siRNA screening has identified CLDN4 and CLDN8 critical for paracellular Cl^- permeability in the collecting duct. Either claudin knockdown cell model phenocopied the other, suggesting these two claudins functioned in the same pathway. This prompted us to ask whether CLDN4 physically interacts with CLDN8. Because mature epithelial cells possess high-order biochemical structures and strong protein-protein interactions within the TJ matrix, which denies an unambiguous study of any selected claudin-claudin interaction, we began with testing CLDN4 and CLDN8 interactions in simple cell systems such as yeast cells and premature epithelial cells that do not form TJs and express no endogenous TJ proteins.

To determine the homo- and heteromeric interactions between CLDN4 and CLDN8, we used a previously described yeast 2-hybrid (Y2H) membrane protein interaction assay in *Saccharomyces cerevisiae* to examine interactions between claudins (*Methods*) (29). Y2H assays revealed strong heteromeric interaction between CLDN4 and CLDN8 by using three different reporter assays (*HIS3*, *lacZ*, and *ADE2*; Fig. 2*A*). CLDN8 showed positive homomeric interaction but CLDN4 failed to interact with itself (Fig. 2*A*). CLDN8 interacted strongly with CLDN3 and CLDN7 (Fig. 2*A*), normal TJ constituents in the collecting duct. *LacZ* reported weak interaction between CLDN4 and CLDN3, but no interaction was evident for the CLDN4/CLDN7 pair on any of our three reporter assays.

To directly document CLDN4-CLDN8 interaction, we attempted coimmunoprecipitation of CLDN4 and CLDN8 in doubly transfected HEK293T cells, an embryonic cell line with no TJ or endogenous claudins. When plated sparsely at low cell density, which minimizes cell-cell contacts and heterotypic interactions, interactions between CLDN4 and CLDN8 will mostly be heteromeric. Immunoblotting showed that anti-CLDN8 antibody coprecipitated CLDN4, whereas anti-CLDN4 antibody reciprocally precipitated CLDN8 (Fig. 2*B*). Other TJ protein antibodies, such as anti-CLDN1 and antioccludin antibody (as nonspecific binding controls), precipitated neither CLDN4 nor CLDN8 (Fig. 2*B*). These biochemical data confirmed heteromeric interactions between CLDN4 and CLDN8 in epithelial cells.

CLDN8 Recruits CLDN4 to the Tight Junction. Knowing that CLDN16-19 interaction is required for their assembly and trafficking into the TJ (19), we asked whether the TJ localization of CLDN4 in the collecting duct cells was directed by its interaction with CLDN8. In the WT collecting duct cells (M-1 or mIMCD3), CLDN4 and CLDN8 were both concentrated in the TJ (Fig. S2*B*). In M-1: CLDN8-siRNA cells, however, CLDN4 staining completely disappeared from TJs (Fig. 3*A*). Intracellular CLDN4 foci were spotted in CLDN8-siRNA cells using confocal microscopy (Fig. 3*A*, arrow). Because polarized epithelia (grown on Transwell) lack the lateral resolution for further microscopic analyses, we were not able to discern the subcellular organelle of CLDN4 localization. Similar CLDN4 mislocalization was found in mIMCD3:CLDN8-siRNA cells. Loss of CLDN4 localization in TJ was not due to reduced CLDN4 expression, because WT and CLDN8-siRNA cells expressed equivalent levels of CLDN4 protein by Western blot (Fig. S2*A*). CLDN4 delocalization was not due to reduced TJ integrity, because CLDN3 and CLDN7 showed normal TJ staining in CLDN8-siRNA cells (Fig. 3*A*), which was indistinguishable from WT cells. Our findings suggest that CLDN4 localization to TJ in the collecting duct is directed by the CLDN4-8 interaction, discussed elsewhere in this study. Unlike the CLDN16-19 interaction that directs the TJ localization of both claudins, CLDN8 localization to TJ of the collecting duct cell (M-1 or mIMCD3) was not affected by absence of CLDN4, nor was CLDN3 or CLDN7 localization. This is compatible with the observation that CLDN8 showed similar strong affinities for CLDN3, 4, and 7 (Fig. 2*A*); loss of CLDN4 did not prohibit CLDN8 binding with other claudins or

Table 2. Paracellular ion conductance in mIMCD3 cells expressing CLDN4 and its charge-neutralizing mutants

Group	Mutation position	TER, Ω·cm^2	Dilution potential, mV	P_{Cl}/P_{Na}	P_{Cl}, 10^{-6} cm/s	P_{Na}, 10^{-6} cm/s	Expression	Localization	Function
mIMCD3	–	476.3 ± 27.8	1.97 ± 0.09	0.766 ± 0.009	1.672 ± 0.011	2.184 ± 0.011	+	TJ	+
mIMCD3:cldn4-siRNA	–	732.7 ± 18.7	8.00 ± 0.17	0.303 ± 0.010	0.582 ± 0.014	1.922 ± 0.014	–	–	–
mIMCD3:cldn4-siRNA+cldn4-WT	–	410.0 ± 3.8	2.63 ± 0.09*	0.699 ± 0.009*	1.841 ± 0.013*	2.635 ± 0.013	+	TJ	+
mIMCD3:cldn4-siRNA+cldn4-R31T	ECL1	591.7 ± 32.9	2.87 ± 0.03*	0.676 ± 0.003*	1.251 ± 0.004*	1.849 ± 0.004	+	TJ	+
mIMCD3:cldn4-siRNA+cldn4-E48Q	ECL1	515.7 ± 5.8	3.03 ± 0.03*	0.661 ± 0.003*	1.415 ± 0.004*	2.142 ± 0.004	+	TJ	+
mIMCD3:cldn4-siRNA+cldn4-K65T	ECL1	389.0 ± 4.7	10.40 ± 0.06†	0.182 ± 0.003**	0.728 ± 0.009†	3.990 ± 0.009†	+	TJ	–
mIMCD3:cldn4-siRNA+cldn4-D68N	ECL1	447.7 ± 9.6	2.53 ± 0.03*	0.709 ± 0.003*	1.699 ± 0.005*	2.398 ± 0.005	+	TJ	+
mIMCD3:cldn4-siRNA+cldn4-D76N	ECL1	433.3 ± 14.2	2.67 ± 0.03*	0.696 ± 0.003*	1.739 ± 0.005*	2.500 ± 0.005	+	TJ	+
mIMCD3:cldn4-siRNA+cldn4-R81T	ECL1	671.0 ± 55.2	8.17 ± 0.03	0.294 ± 0.002	0.621 ± 0.003	2.114 ± 0.003	Weak	ER	–

CLDN4-siRNA: 282.

*$P < 0.01$ relative to CLDN4-siRNA, $n = 3$.

†$P < 0.01$ relative to CLDN4-WT, $n = 3$.

CELL BIOLOGY

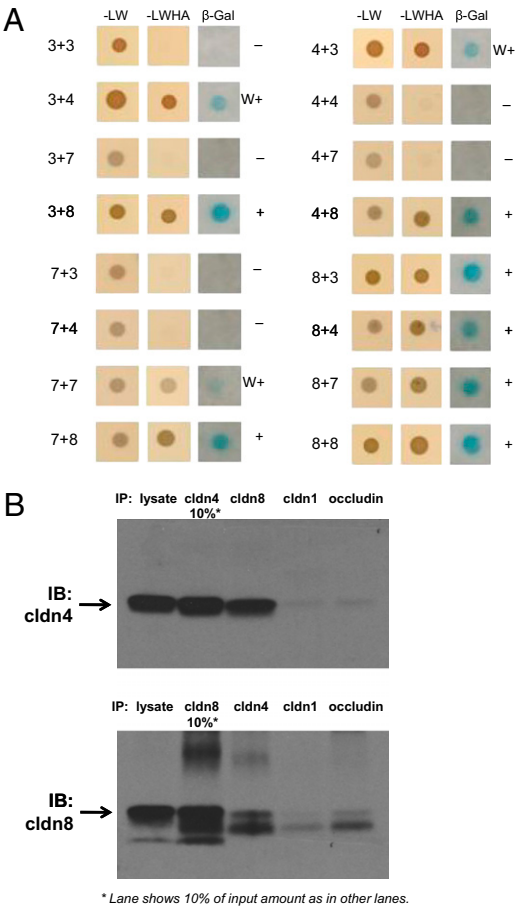

Fig. 2. CLDN4 interacts with CLDN8. (*A*) Y2H assays showing interaction of CLDN4 with CLDN8, determined by using three reporter genes (*HIS3*, *lacZ*, and *ADE2*) in the yeast NMY51 strain. CLDN8 also interacts strongly with itself and with CLDN3 and CLDN7. Shown are plates with selective medium lacking leucine and tryptophan (SD-LW), indicating the transforming of both bait and prey vectors; with SD-LWHA, indicating the expression of reporter genes *HIS3* and *ADE2*; and the β-galactosidase assay. (*B*) Coimmunoprecipitation of CLDN4 and CLDN8 cotransfected in HEK293T cells. Antibodies used for coimmunoprecipitation are shown above the lanes; antibody for blot visualization is shown at left.

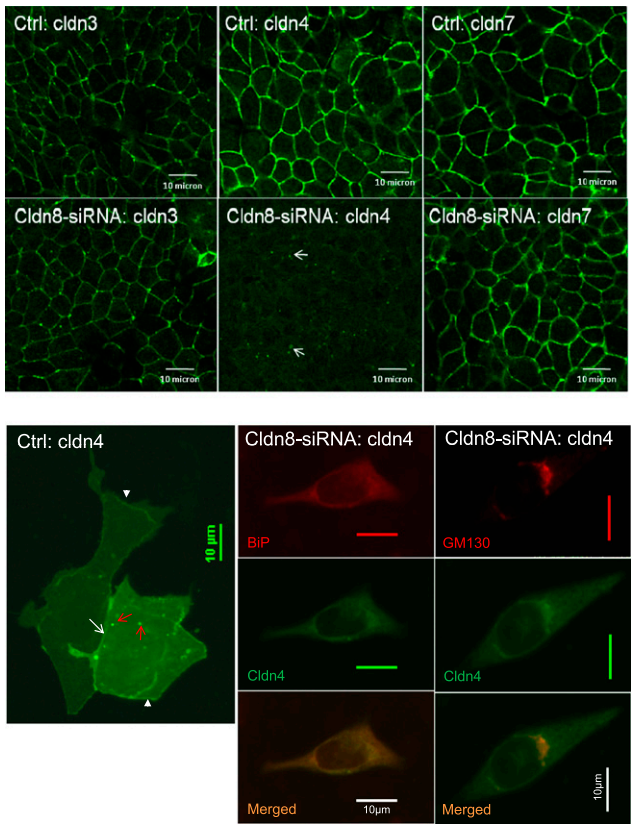

Fig. 3. CLDN4 delocalization in CLDN8-siRNA cells. (*A*) In polarized M-1 cells (shown as representative), CLDN4 is mislocalized to the cytoplasm (arrow) in the absence of CLDN8. CLDN3 or CLDN7 TJ localization is not dependent on CLDN8. (*B*) In subconfluent, not fully polarized, M-1 cells, CLDN4 is localized predominantly at sites of cell-cell interaction (green arrow), variably at the nonjunctional plasma membrane (green arrowhead) and occasionally in traveling intracellular vesicles (red arrow). In the absence of CLDN8, CLDN4 is confined to the ER (counterstained with anti-BiP antibody) and the Golgi apparatus (counterstained with anti-GM130 antibody).

its assembly to TJ. CLDN4 demonstrated a higher affinity for CLDN8 than for either CLDN3 or CLDN7 (Fig. 2*A*); loss of CLDN8, the only functional binding partner for CLDN4, rendered its disassembly and delocalization from TJ.

Integral multimeric membrane proteins generally oligomerize in the endoplasmic reticulum (ER) (31) and in the Golgi apparatus (32); it is likely that CLDN4 and CLDN8 follow this pattern. In subconfluent, not fully polarized WT M-1 cells, CLDN4 localized predominantly at sites of cell-cell interaction (Fig. 3*B Left*, white arrow) and variably at the nonjunctional plasma membrane (Fig. 3*B Left*, white arrowhead). Occasionally, CLDN4 was found in traveling intracellular vesicles (Fig. 3B *Left*, red arrow). In M-1:CLDN8-siRNA cells, however, CLDN4 was sequestered within the ER showing a reticular cytoplasmic and perinuclear distribution (Fig. 3*B Right*, counterstained with an ER marker—BiP)m and within the Golgi apparatus seen as tubular structures close to the periphery of the nucleus (Fig. 3*B Right*, counterstained with a Golgi apparatus marker—GM130). To selectively rescue the loss of CLDN8 function in M-1 cells and test for its role in CLDN4 trafficking, we stably expressed the siRNA-resistant human CLDN8, which contains six mismatches to the mouse siRNA sequence (714), and tracked the subcellular localization of both claudins. In M-1:CLDN8-siRNA cells rescued with human CLDN8, CLDN4 mislocalization was corrected and restored to the same pattern as in WT cells. It was found both at the plasma membrane (Fig. S4 *Center*, green arrow) and in traveling intracellular vesicles (Fig. S4 *Center*, green arrowhead) to be colocalized with CLDN8 (Fig. S4 *Right*, yellow arrow and arrowhead). CLDN4 cotrafficked with CLDN8 and depended upon CLDN8 for recruitment to the plasma membrane. Notably, some CLDN8-abundant vesicles lacked CLDN4 staining (Fig. S4 *Left*, red arrowhead). The absence of a correlation between CLDN8 and CLDN4 staining in these vesicles indicated that CLDN8 had additional binding partners, e.g., CLDN3 and 7. We also examined the localization patterns of CLDN4 and the effects of CLDN8 on CLDN4 localization in mIMCD3:CLDN8-siRNA cells and confirmed our findings in M-1:CLDN8-siRNA cells.

Discussion

In this study, we show that CLDN4 and CLDN8, two proteins that are required for paracellular reabsorption of Cl^-, interacted in cell membranes. The interaction was supported by four independent lines of evidence: (*i*) a positive Y2H assay; (*ii*) coimmunoprecipitation in epithelial cells; (*iii*) cotrafficking and colocalization in epithelial cells; and (*iv*) CLDN8 recruitment of CLDN4 to TJs. Collecting duct cell models deficient in either claudin developed paracellular loss of Cl^-, emphasizing the functional importance of CLDN4-8 heteromeric interaction in the trafficking and polymerizing of CLDN4, the paracellular Cl^- channel, although the TJ localization of CLDN8 may not depend upon this interaction.

The molecular mechanisms of NaCl reabsorption vary along the different segments of the ASDN. In the DCT, Na^+ and Cl^- are cotransported by the thiazide-sensitive NaCl cotransporter NCC. In contrast with the DCT, the reabsorption of Na^+ is molecularly separated from that of Cl^- in the collecting duct. Na^+ reabsorption

occurs through the principal cell via the epithelial sodium channel (ENaC), whereas Cl^- reabsorption is mediated predominantly (~70%) through the paracellular pathway and to a lesser extent through the β-type intercalated cell via the Cl^-/HCO^- exchanger pendrin (33). The driving force for paracellular Cl^- reabsorption is the large lumen-negative transepithelial potential (V_{te}: ~ –25mV; Fig. S5). V_{te} is generated by the unidirectional transepithelial Na^+ current (lumen to bath) and is sufficient to overcome the transepithelial Cl^- concentration gradient that would otherwise favor Cl^- secretion. The level of transepithelial Cl^- reabsorption must match that of Na^+ reabsorption so as to maintain luminal fluid electroneutrality. Defects in paracellular Cl^- shunt increase the magnitude of V_{te}, depolarize the luminal membrane, and subsequently inhibit ENaC. The presence of paracellular Cl^- conductance has long been revealed by a number of elegant in vitro studies using microdissected perfused collecting duct tubules (24, 33–35). The paracellular Cl^- conductance was estimated to be near 1.0 mS/cm^2 using perfused rabbit cortical collecting ducts (34). Here, we have identified CLDN4 as the underlying molecular component of paracellular Cl^- shunt. The baseline levels of Cl^- conductance in our measurements were close to those from previous perfusing experiments: 1.38 mS/cm^2 for M-1 cells and 1.61 mS/cm^2 for mIMCD3 cells. Loss of CLDN4 significantly reduced paracellular Cl^- conductance in these cultured collecting duct cells (M-1 KD: 0.72 mS/cm^2; mIMCD3 KD: 0.41 mS/cm^2). The CLDN4 responsible Cl^- conductance was 0.66 mS/cm^2 in M-1 cells and 1.20 mS/cm^2 in mIMCD3 cells. Stoos et al. (20) have recorded the amiloride-sensitive Na^+ current in M-1 epithelia and estimated the ENaC mediated Na^+ conductance to be 0.63 mS/cm^2. Thus, the molecular mechanism for coupling Cl^- transport with Na^+ transport in the collect duct is provided by the CLDN4 paracellular channel. The significance of paracellular Cl^- reabsorption in blood pressure control has been demonstrated in two recent studies. Yamauchi et al. (36) and Kahle et al. (37) have shown, WNK4, causing the inherited hypertensive disease pseudohypoaldosteronism type II (PHAII) syndrome, selectively increases paracellular Cl^- permeability in MDCK cells and phosphorylates claudins, including CLDN4. Aldosterone, the primary blood pressure-regulating hormone, upregulates paracellular Cl^- permeability in a rat cortical collecting duct cell line RCCD2 and hyperphosphorylates CLDN4 (38). Although we have not studied the regulation of CLDN4 channel, claudin phosphorylation was demonstrated by Ikari et al. (39) to play important roles in targeting claudin-16 to TJ. CLDN4 KO animal studies are currently under way to elucidate the in vivo role of CLDN4 in blood pressure control.

For additional discussion, see *SI Discussion*.

Methods

See *SI Methods* for additional information on the following topics: reagents, antibodies, cell lines, animals, siRNA screening, molecular cloning, retrovirus production, protein electrophoresis, immunoblotting, coimmunoprecipitation, immunolabeling, confocal microscopy, Y2H membrane protein interaction assay, electrophysiological measurements, inhibitors of transcellular ion transport, and statistical analyses. The animal studies were approved by the Institutional Ethical Committee for the Care of Animals.

ACKNOWLEDGMENTS. We thank Dr. Daniel Goodenough (Harvard Medical School) for thoughtful insights and suggestions on this work. This work was supported by National Institutes of Health Grants RO1DK084059 and P30 DK079333 (to J.H.), American Heart Association Grant 0930050N (to J.H.), and Deutsche Forschungs Gemeinschaft SFB-593 and P. E. Kempkes Foundation Grant 10/08 (to A.R).

1. Kurtz TW, Morris RC, Jr (1983) Dietary chloride as a determinant of "sodium-dependent" hypertension. *Science* 222:1139–1141.
2. Tanaka M, Schmidlin O, Yi SL, Bollen AW, Morris RC, Jr (1997) Genetically determined chloride-sensitive hypertension and stroke. *Proc Natl Acad Sci USA* 94:14748–14752.
3. Whitescarver SA, Ott CE, Jackson BA, Guthrie GP, Jr, Kotchen TA (1984) Salt-sensitive hypertension: Contribution of chloride. *Science* 223:1430–1432.
4. Lifton RP, Gharavi AG, Geller DS (2001) Molecular mechanisms of human hypertension. *Cell* 104:545–556.
5. Wall SM (2005) Recent advances in our understanding of intercalated cells. *Curr Opin Nephrol Hypertens* 14:480–484.
6. Canessa CM, et al. (1994) Amiloride-sensitive epithelial Na+ channel is made of three homologous subunits. *Nature* 367:463–467.
7. Royaux IE, et al. (2001) Pendrin, encoded by the Pendred syndrome gene, resides in the apical region of renal intercalated cells and mediates bicarbonate secretion. *Proc Natl Acad Sci USA* 98:4221–4226.
8. Tsukita S, Furuse M, Itoh M (1996) Molecular dissection of tight junctions. *Cell Struct Funct* 21:381–385.
9. Furuse M, Fujita K, Hiiragi T, Fujimoto K, Tsukita S (1998) Claudin-1 and -2: Novel integral membrane proteins localizing at tight junctions with no sequence similarity to occludin. *J Cell Biol* 141:1539–1550.
10. Tsukita S, Furuse M (2000) Pores in the wall: Claudins constitute tight junction strands containing aqueous pores. *J Cell Biol* 149:13–16.
11. Tang VW, Goodenough DA (2003) Paracellular ion channel at the tight junction. *Biophys J* 84:1660–1673.
12. Kiuchi-Saishin Y, et al. (2002) Differential expression patterns of claudins, tight junction membrane proteins, in mouse nephron segments. *J Am Soc Nephrol* 13:875–886.
13. Li WY, Huey CL, Yu AS (2004) Expression of claudin-7 and -8 along the mouse nephron. *Am J Physiol Renal Physiol* 286:F1063–F1071.
14. Tatum R, et al. (2010) Renal salt wasting and chronic dehydration in claudin-7-deficient mice. *Am J Physiol Renal Physiol* 298:F24–F34.
15. Van Itallie C, Rahner C, Anderson JM (2001) Regulated expression of claudin-4 decreases paracellular conductance through a selective decrease in sodium permeability. *J Clin Invest* 107:1319–1327.
16. Yu AS, Enck AH, Lencer WI, Schneeberger EE (2003) Claudin-8 expression in Madin-Darby canine kidney cells augments the paracellular barrier to cation permeation. *J Biol Chem* 278:17350–17359.
17. Alexandre MD, Lu Q, Chen YH (2005) Overexpression of claudin-7 decreases the paracellular Cl^- conductance and increases the paracellular Na^+ conductance in LLC-PK1 cells. *J Cell Sci* 118:2683–2693.
18. Piontek J, et al. (2008) Formation of tight junction: Determinants of homophilic interaction between classic claudins. *FASEB J* 22:146–158.
19. Hou J, et al. (2009) Claudin-16 and claudin-19 interaction is required for their assembly into tight junctions and for renal reabsorption of magnesium. *Proc Natl Acad Sci USA* 106:15350–15355.
20. Stoos BA, Náray-Fejes-Tóth A, Carretero OA, Ito S, Fejes-Tóth G (1991) Characterization of a mouse cortical collecting duct cell line. *Kidney Int* 39:1168–1175.
21. Zhang W, et al. (2007) Aldosterone-induced Sgk1 relieves Dot1a-Af9-mediated transcriptional repression of epithelial Na^+ channel alpha. *J Clin Invest* 117:773–783.
22. Hou J, Gomes AS, Paul DL, Goodenough DA (2006) Study of claudin function by RNA interference. *J Biol Chem* 281:36117–36123.
23. Hou J, Paul DL, Goodenough DA (2005) Paracellin-1 and the modulation of ion selectivity of tight junctions. *J Cell Sci* 118:5109–5118.
24. O'Neil RG, Sansom SC (1984) Electrophysiological properties of cellular and paracellular conductive pathways of the rabbit cortical collecting duct. *J Membr Biol* 82:281–295.
25. Eisenman G, Horn R (1983) Ionic selectivity revisited: The role of kinetic and equilibrium processes in ion permeation through channels. *J Membr Biol* 76:197–225.
26. Colegio OR, Van Itallie C, Rahner C, Anderson JM (2003) Claudin extracellular domains determine paracellular charge selectivity and resistance but not tight junction fibril architecture. *Am J Physiol Cell Physiol* 284:C1346–C1354.
27. Yu AS, et al. (2009) Molecular basis for cation selectivity in claudin-2-based paracellular pores: Identification of an electrostatic interaction site. *J Gen Physiol* 133:111–127.
28. Furuse M, Sasaki H, Tsukita S (1999) Manner of interaction of heterogeneous claudin species within and between tight junction strands. *J Cell Biol* 147:891–903.
29. Hou J, et al. (2008) Claudin-16 and claudin-19 interact and form a cation-selective tight junction complex. *J Clin Invest* 118:619–628.
30. Hou J, et al. (2007) Transgenic RNAi depletion of claudin-16 and the renal handling of magnesium. *J Biol Chem* 282:17114–17122.
31. Hurtley SM, Helenius A (1989) Protein oligomerization in the endoplasmic reticulum. *Annu Rev Cell Biol* 5:277–307.
32. Musil LS, Goodenough DA (1993) Multisubunit assembly of an integral plasma membrane channel protein, gap junction connexin43, occurs after exit from the ER. *Cell* 74:1065–1077.
33. Sansom SC, Weinman EJ, O'Neil RG (1984) Microelectrode assessment of chloride-conductive properties of cortical collecting duct. *Am J Physiol* 247:F291–F302.
34. Warden DH, Schuster VL, Stokes JB (1988) Characteristics of the paracellular pathway of rabbit cortical collecting duct. *Am J Physiol* 255:F720–F727.
35. O'Neil RG, Boulpaep EL (1982) Ionic conductive properties and electrophysiology of the rabbit cortical collecting tubule. *Am J Physiol* 243:F81–F95.
36. Yamauchi K, et al. (2004) Disease-causing mutant WNK4 increases paracellular chloride permeability and phosphorylates claudins. *Proc Natl Acad Sci USA* 101: 4690–4694.
37. Kahle KT, et al. (2004) Paracellular Cl^- permeability is regulated by WNK4 kinase: Insight into normal physiology and hypertension. *Proc Natl Acad Sci USA* 101: 14877–14882.
38. Le Moellic C, et al. (2005) Aldosterone and tight junctions: Modulation of claudin-4 phosphorylation in renal collecting duct cells. *Am J Physiol Cell Physiol* 289: C1513–C1521.
39. Ikari A, et al. (2006) Phosphorylation of paracellin-1 at Ser217 by protein kinase A is essential for localization in tight junctions. *J Cell Sci* 119:1781–1789.